Ultrasonics Sonochemistry 91 (2022) 106230

Contents lists available at ScienceDirect

Ultrasonics Sonochemistry

journal homepage: www.elsevier.com/locate/ultson

Fabrication of icariin-soymilk nanoparticles with ultrasound-assisted treatment

Jinping Wang [a,d], Hong Zhu [a,b,c], Yueming Jiang [a,b,c], Jianbo Xiao [e], Bao Yang [a,b,c,*], Lingrong Wen [a,b,*]

[a] Guangdong Provincial Key Laboratory of Applied Botany, Key Laboratory of South China Agricultural Plant Molecular Analysis and Genetic Improvement, South China Botanical Garden, Chinese Academy of Sciences, Guangzhou 510650, China
[b] South China National Botanical Garden, Guangzhou 510650, China
[c] University of Chinese Academy of Sciences, Beijing 100049, China
[d] College of Food Science and Engineering, Jilin Agricultural University, Changchun 130118, China
[e] Faculty of Food Science and Technology, University of Vigo, Ourense E-32004, Spain

ARTICLE INFO

Keywords:
Bioavailability
Hydrophobic interaction
Microstructure
NMR
Cryo-SEM

ABSTRACT

Ultrasound is effective to fabricate nanocomplex. Soymilk is a natural nanocarrier with good compatibility. However, information about soymilk-nutraceuticals nanocomplex is limited. In this work, soymilk was used to encapsulate icariin, a well known nutraceutical with poor bioavailability. The effect of ultrasound on the quality of icariin-soymilk nanocomplexes (ISNCs) was investigated. Ultrasound could reduce the particle size, improve the surface hydrophobicity and change the microstructure of soymilk. With increasing ultrasound treatment time, an increased surface hydrophobicity was observed. The highest encapsulation efficiency (89.67 %) and loading capacity (28.92 μg/mg) were found for USI-20, whereas the smallest particle size (132.47 nm) was observed for USI-120. USI-60 showed the lowest ζ-potential (-31.33 mV) and the highest bioaccessibility (76.08 %). Ultrasound could enhance the storage stability of ISNCs. The data of NMR and fluorescence indicated that ISNCs were mainly stabilized by hydrophobic interaction.

1. Introduction

Epimedium is a vital traditional Chinese medicinal herb, which is a well-known botanical supplement widely used in diversified traditional Chinese formulations, modern proprietary Chinese medicine products and functional foods due to the efficacy on cardiovascular disease, osteoporosis and immunoregulation [1]. Icariin is a characteristic bioactive compounds in *Epimedium*. Recently, icariin has gained popularity due to a range of health-promoting properties, including preventing osteoporosis, osteoarthritis, erectile dysfunction, cancer and depression, modulating the immune and nervous system and improving cardiovascular function, as well as its safety to human being [1,2]. Icariin shows promising potential for acting as nutraceutical in functional foods [3]. However, the utilization of icariin is limited due to its high hydrophobicity and poor oral bioavailability [4]. Several strategies, including pharmaceutical technologies (complex formation with phospholipids, cyclodextrins, nanotechnologies (formation of micelles, nano-carrier, nanogels, nano-crystals, and microspheres), structural transformation and absorption enhancement have been developed to improve the bioavailability of icariin [3]. However, the low solubility in aqueous matrix and poor bioavailability of icariin in these systems have not been solved. Therefore, more efficient delivery systems are required to be developed.

Soymilk is a stable emulsion composed of proteins, carbohydrates, fats, vitamins and minerals. Soymilk has reported to be an effective emulsifier that possessed encapsulating effect on bioactive substances [5]. Additionally, previous study indicated that curcumin could be successfully loaded into bovine milk and the storage stability and *in vitro* bioavailability of curcumin were improved [6]. As a dairy milk, the components of soymilk are similar to bovine milk, suggesting that soymilk may develop as nano-carrier for bioactive substances.

Ultrasound can modify food proteins and improve their functional properties in the food industry. Previous study showed that ultrasound could change the emulsification, solubility and thermal gelation of soy

* Corresponding authors at: Guangdong Provincial Key Laboratory of Applied Botany, Key Laboratory of South China Agricultural Plant Molecular Analysis and Genetic Improvement, South China Botanical Garden, Chinese Academy of Sciences, Guangzhou 510650, China.
E-mail addresses: yangbao@scbg.ac.cn (B. Yang), wenlingrong@scbg.ac.cn (L. Wen).

https://doi.org/10.1016/j.ultsonch.2022.106230
Received 29 September 2022; Received in revised form 14 November 2022; Accepted 18 November 2022
Available online 19 November 2022

protein isolate (SPI) [7]. Previous study also indicated that ultrasound could improve functional properties of soymilk [8]. Additionally, secondary structures changes were observed in ultrasound treated-soymilk [9]. More hydrophobic groups of soybean proteins could be exposed to the interface after ultrasound treatment since ultrasound can change the tertiary structure of proteins [10]. These improvements may favor the nano-complexation. Previous study also pointed out that ultrasound could improve the encapsulation efficiency of bioactive substances in a protein-base nano-complex [11]. Ultrasound have been proven to be positive in proteins, which act as emulsion stabilizers, nano-carriers or bulk gel matrix of bioactive compounds. However, the effect of ultrasound treatment on soymilk as a nano-carrier has not been elucidated.

Therefore, this study aimed to analyze the effects of ultrasound treatment on physicochemical properties, chemical compositions, microstructure and secondary structure of soymilk. Furthermore, the influences of ultrasound on the formation and properties of icariin-soymilk nanocomplexes (ISNCs), including particle size distribution, ζ-potential, microstructure, stability and bioavailability were characterized. Furthermore, the interaction force involved in ISNCs were investigated by nuclear magnetic resonance (NMR) and fluorescent spectrometry. This study could supply useful information to construct icariin nanocomplexes using soymilk as a natural carrier.

2. Materials and methods

2.1. Materials

Sodium chloride (99.5 %) and icariin (96 %) were provided by Shanghai Aladdin Biochemical Technology Co., ltd (Shanghai, China). The soybeans were purchased from Wuchang Caiqiao Rice Industry Co., ltd. (Harbin, China). 8-Anilino-1-naphthalenesulfonicate (ANS-Na) was obtained from Shanghai Macklin Biochemical Co., ltd (Shanghai, China). Bovine serum albumin and Folin-Ciocalteau reagents were obtained from Sigma-Aldrich (St. Louis, MO, USA). Sodium hydroxide (≥96.0 %), hydrochloric acid (36.0–38.0 %), disodium hydrogen phosphate dodecahydrate (≥99.0 %) and sodium dihydrogen phosphate dihydrate (≥99.0 %) were provided by Guangzhou chemical reagent factory (Guangzhou, China). All the other chemical reagents were of analytical grade.

2.2. Preparation of soymilk

A total of 100-g soybeans were washed with deionized water and were ground with 1300 mL of deionized water using a cell wall breaker (L18-Y933, Joyoung Household Electrical Appliances Co., Ltd., Jinan, China) for 39 min. The slurry was quickly cooled to room temperature using an iced water bath. The supernatant was collected for subsequent analysis after centrifugation at 5000 *g* for 30 min at 25 °C.

2.3. Ultrasound treatment

The soymilk was treated with an Ultrasound Cell Disrupter (VCX 750, Sonics & Materials, Inc. New town, USA) equipped with a grade titanium alloy probe (13 mm high). Briefly, soymilk were treated for 20, 60 and 120 min under ultrasound condition with a titanium alloy probe dipping (approximately 2.0 cm) into the samples. Soymilk samples with different treating time represented as US-20, US-60 and US-120, respectively. The ultrasound conditions were as follows: the on-time and off-time of the pulsed ultrasound was 3.0 and 2.0 s, respectively. The ultrasound power, frequency and amplitude were 750 W, 20 kHz and 40 %, respectively. Untreated soymilk (NS) was used as control. During the ultrasound process, the temperature was controlled below 25 ± 1 °C using an ice-water bath. After treatment, the soymilk was incubated at 4 °C before further analysis.

2.4. Determination of protein and total carbohydrates contents

Protein content was measured by Lowry method using bovine serum albumin as the standard [12]. The final result was calculated as milligrams of bovine serum albumin equivalents per gram of soymilk (mg BSAE/g).

The total carbohydrate contents were measured by phenol–sulfuric acid protocol [13]. Briefly, 1.0 mL of fresh made soymilk was mixed thoroughly with 0.5 mL of phenol solution (6 %, w/w) in a test tube. After the addition of 3.0 mL concentrated sulfuric acid, the test tube was shook immediately and the mixture was incubated at room temperature for 30 min. The absorbance was measured at 490 nm using a multifunctional microplate reader (Spark, Tecan Group Ltd., Männedorf, Switzerland). The content of total carbohydrate was finally calculated as milligram of glucose equivalents per gram soymilk (mg GE/g) using glucose as the standard.

2.5. Determination of total amino acids

The amino acid composition of treated and untreated soymilk were measured following the protocol of previous report [14]. In brief, 100 mg of freeze-dried soymilk powder were hydrolyzed by 6 M HCl at 110 °C for 23 h. Notely, methionine and cystine were hydrolyzed after pre-treating with performic acid oxidation. The contents were determined by S-433 (D) Automatic Amino Acid Analyzer (Sykam Co. ltd, Eresing, Germany), which was equipped with an ion exchange column (LCA K-07/Li 4.6 × 150 mm). The solution was eluted with solvent A (120 mM lithium citrate, pH 2.9), solvent B (300 mM lithium citrate, pH 8.0) and solvent C (200 mM lithium citrate, pH 4.2). The amino acid content in tested sample was determined on the basis of the peak area of the detected amino acid with that of the corresponding standard.

2.6. Surface hydrophobicity (H_o)

H_o of soymilk was measured by the ANS-Na method. Briefly, freeze-dried soymilk powder was dissolved in PBS (10 mM, pH 7.0) to obtain a series sample with concentration ranges of 0.01 to 1 mg/mL. Then the tested sample (4 mL) were incubated with ANS-Na solution (8.0 mM, 50 μL). ANS-Na in PBS was used as blank control. Soy protein isolate (SPI) at the same concentrations was analyzed for comparison. After reaction in the dark for 5 min, the relative fluorescent intensity was determined by using a multifunctional microplate reader (excitation, 370 nm and emission, 465 nm). H_o was defined as the initial slope of the curve of relative fluorescence intensity versus soymilk concentrations using the linear regression analysis.

2.7. Circular dichroism (CD)

Soymilk powder was dissolved in deionized water to a final concentration of 0.1 mg/mL. CD scanning was performed with wavelength range of 190–260 nm, band-width of 1.0 nm, speed of 100 nm/min, and response time of 1.0 s. The content of secondary structure, including α-helix, β-turn, β-sheet and random coil was calculated after recording the CD spectrum at 25 °C. Deionized water was used as the blank control.

2.8. Nanocomplexes preparation

Icariin (5 mg/mL) was dissolved in 70 % ethanol (v/v). Under stirring at 400 rpm, icariin solution was added dropwisely to soymilk in a ratio of 1:5 (v/v) under stirring using a magnetic stirrer (RT 5, IKA®, Werke GmbH & Co., Staufen, Germany). Icariin-soymilk complexes was obtained after the above mixture was stirred continuously at room temperature for 1 h. ISNCs were collected after centrifugation (10000 *g*, 15 min). The final ISNCs were named as NSI, USI-20, USI-60 and USI-120, respectively, in accordance with the corresponding soymilk.

2.9. Characterization of ISNCs

2.9.1. Encapsulation efficiency (EE) and loading capacity (LC)

The free icariin was collected after centrifugation (10000 *g*, 15 min), and was mixed with anhydrous ethanol. The content of icariin was determined at 360 nm with an ultrahigh performance liquid chromatography (UHPLC, Agilent technologies, UPLC, 1260, Waldbronn, Germany). A Hypersil GOLD^{TM} threaded column (2.1 × 100 mm, Thermo Fisher Scientific (China) Co., ltd., Shanghai, China) was used. The injection volume and flow rate were 2.0 μL and 0.4 mL/min, respectively. The elution gradient of solvent A (H_2O) and solvent B (acetonitrile) was set as: 3 % B (0.0–3.0 min); 3 %-95 % B (3.0–15.0 min); 95 % B (15.0–20.0 min); 95 %-3% B (20.0–20.5 min); 3 % B (20.5–25.0 min). The standard calibration curve was established using icariin solution in a 0.05–1.0 mg/mL concentration range. The EE and LC values of icariin were calculated as follows:

$$EE(\%) = m_e/m_i \times 100 \quad (1)$$

$$LC\ (\mu g/mg) = m_e/m \times 100 \quad (2)$$

Where m_e and m_i are the contents of encapsulated icariin and the initial icariin used, respectively. In addition, m represents the total mass of ISNCs.

2.9.2. Particle size, polydispersity index (PDI) and ζ-potential

The particle size, ζ-potential and polydispersity index (PDI) of the soymilk and ISNCs were determined at 25 °C using a Nanosizer ZS instrument (Nano-ZS, Malvern Instruments Co. ltd., Worcestershire, UK), and a He-Ne laser operation at 633 nm was used. After diluting to a concentration of 1 % (w/v) with deionized water, the prepared samples were measured in triplicate at 25 °C.

2.9.3. Cryo-scanning electron microscopy (Cryo-SEM)

The morphology of icariin, soymilk and ISNCs were observed by Cryo-SEM (Hitachi Regulus 8100, Japan). Before transferring to the preparation chamber by vacuum transfer system for fracture and sublimation, 10 μL of sample solutions were quickly cooled in liquid nitrogen. Then the samples were coated with Pt, and were transferred to the SEM chamber for observation at an acceleration voltage of 10 kV.

2.10. Formation mechanism of ISNCs

2.10.1. NMR analysis

An NMR spectrometer (DRX-500, Bruker, Rheinstetten, Germany) was used to determine the interaction between icariin and soymilk [15]. The heteronuclear single quantum coherence spectroscopy (HSQC) and ^1H and spectra of icariin in DMSO-d_6, soymilk and ISNCs in both DMSO-d_6 and D_2O were recorded at 25 °C, respectively. In D_2O, acetone (δ ^1H 2.22 ppm and ^{13}C 30.89 ppm) was used as internal standard.

2.10.2. Fluorescent spectrometry analysis

ISNCs were freshly prepared with the final concentrations of icariin were 0, 10, 20, 30, 40 and 50 μM, respectively. After incubation in a constant-temperature water bath for 30 min, at 298, 303 and 308 K, respectively, the fluorescence intensity of the mixture was measured by a fluorescence spectrophotometer (F-7000, Hitachi, Tokyo, Japan) with an excitation wavelength of 280 nm and emission wavelengths of 300–450 nm.

The following Stern-Volmer equation was used for calculation to reflect the parameters correlated with the quenching mechanism of soymilk.

$$F_0/F = 1 + K_q\tau_0[Q] = 1 + K_{SV}[Q] \quad (3)$$

$$\lg\left[(F_0 - -F)/F\right] = \lg K_A + n\lg[Q] \quad (4)$$

In which *F* and F_0 are the fluorescence intensity in the presence and absence of icariin, respectively; τ_0 refers to the average fluorescence lifetime without quencher and equals = 10^{-8} s; K_q refers to the quenching constant ($M^{-1}S^{-1}$); [Q] refers to the concentration of icariin; K_A refers to the binding constant; K_{SV} refers to the Stern-Volmer quenching constant, M^{-1}; n is the number of binding sites.

Van't Hoff equation and thermodynamic equation were used to calculate the thermodynamic parameters involved in binding mechanism between soymilk and icariin.

$$\ln K_A = -(\Delta H/RT) + \Delta S/R \quad (5)$$

$$\Delta G = \Delta H - - T\Delta S \quad (6)$$

In which ΔS, ΔH and ΔG refer to the change of entropy, enthalpy and Gibbs free energy, respectively; T refers to experimental temperature; and R (8.314 J $mol^{-1}\cdot K^{-1}$) refers to ideal gas constant.

2.11. Nanocomplexes stability

2.11.1. Ionic strength and pH stability

NaCl was added into freshly prepared ISNCs to obtain final salt concentrations of 0–1000 mM. Additionally, the pH of the freshly prepared ISNCs were adjusted to 2.0–12.0 using 0.1 M HCl or 0.1 M NaOH. Then the stability was evaluated by measuring the ζ-potential and particle size after keeping at 4 °C for 24 h.

2.11.2. Storage stability

The freshly prepared ISNCs were stored at 25 or 4 °C for 28 days, followed by the particle size and ζ-potential determination every 7 days.

2.11.3. Thermal stability

The freshly prepared ISNCs were incubated in an HWS-26 water bath (Yiheng Scientific Instrument Co., ltd, Shanghai, China) at 25, 60 and 90 °C, respectively, for 120 min. After cooling to room temperature with ice water, the mixture was centrifuged (10000 *g*, 15 min, 25 °C) and the supernatants were collected. The content of icariin in the supernatant was determined as described above by UHPLC. The remaining rate (%) of icariin was calculated as following:

$$Remaining\ rate\ (\%) = m_A/m_T \times 100 \quad (7)$$

Where m_A is the content of icariin in the supernatant after thermal treatment and m_T is the total content of icariin in the whole system before thermal treatment.

2.12. In vitro gastrointestinal digestion

The simulated gastrointestinal tract (GIT) model used in the present work was described previously [16], with some modifications. First, all the samples were placed in Erlenmeyer flasks and then kept at 37 °C in a shaker (HZQ-F160A, Yiheng Scientific Instrument Co., ltd, Shanghai, China) for 10 min at a shaking rate of 100 rpm for preheating treatment. Free icariin in water was used as a control.

Stomach phase: Briefly, 20 mL of samples were adjusted to pH 2.0 using HCl (1.0 M). The solution was then mixed with pepsin (4 % w/w, on dry matter base) and reacted at in a shaker (100 rpm/min, 37 °C) for 60 min.

Intestine phase: The pH of the mixture from the stomach phase was adjusted back to pH 7.0 by using NaOH (2.0 M). Subsequently, trypsin (4 % w/w, on dry matter base) and bile salts (0.5 %, w/v) were added. Then the mixture was stirred (37 °C, 100 rpm/min) for 120 min for intestinal digestion.

The particle size distribution of ISNCs and free icariin throughout the simulated GIT were measured. The bioaccessibility of icariin after the small intestinal phase was measured as described by Chen et al. [15]. The bioaccessibility of icariin were calculated using the following equation:

$$Bioaccessibility(\%) = m_s/m_0 \times 100 \quad (8)$$

Where, m_s and m_0 refers to the contents of icariin in the centrifuged samples after digestion and the initial mass of icariin in ISNCs.

2.13. Statistical analyses

All the data were expressed as mean ± standard deviation (SD). The statistical significance of the data was determined using One-way analysis of variance (ANOVA) followed by T-test to determine the statistical differences between independent samples. And $p < 0.05$ indicated a significant difference.

3. Results and discussions

3.1. Effect of ultrasound treatment on the chemical composition of soymilk

Proteins, carbohydrates and amino acids are the major chemicals in soymilk. The protein level of NS was 25.24 mg/g, which were 25.19, 25.00 and 23.97 mg/g in US-20, US-60 and US-120, respectively. Similarly, the total carbohydrate contents of NS, US-20, US-60 and US-120 were 86.73, 86.49, 86.36 and 86.32 mg/g, respectively (Fig. 1A). No significant differences were observed in the protein and total carbohydrate contents of all the tested soymilks ($p > 0.05$). Similar phenomenon was observed in the total amino acids contents of the tested soymilks (Table S1). All these results indicated that no obvious effects on the chemical compositions were induced by ultrasound treatment. Among the 17 amino acids analyzed, glutamic acid was the predominant amino acid in soymilk, with the contents ranging from 3.33 to 3.54 mg/g, followed by aspartic acid and arginine. It was worth noting that soymilk was rich in hydrophobic amino acids, which had the ability to bind to other hydrophobic molecules to form stable complex by non-covalent interactions [17]. The hydrophobic amino acids like methionine, leucine, isoleucine, valine, phenylalanine, alanine and proline accounted for 34.02, 33.91, 34.05 and 34.70 % of the total amino acids in NS, US-20, US-60 and US-120, respectively. It suggested that soymilk was potent as delivery system of bioactive compounds.

3.2. Effect of ultrasound treatment on H_o

H_o was applied to monitor the effect of ultrasound on the tertiary structure of soymilk. The H_o values of ultrasound-treated soymilk for different time are shown in Fig. 1B. Compared to NS, the H_o value of ultrasound-treated soymilk increased along with increased time. The H_o values of NS, US-20, US-60 and US-120 were 7106.43, 7141.80, 7638.20 and 9902.57, respectively. Similar phenomenon has been observed in wheat gluten and myosin [18]. However, there were no significant ($p > 0.05$) differences among NS, US-20 and US-60. The above results implied that some of the hydrophobic regions of soybean proteins could be exposed to the surface due to the cavitation phenomenon induced by ultrasound treatment. In addition, the H_o value of US-120 was significantly higher ($p < 0.05$) than that of SPI (7725.03), which was a well-known nano-carrier of bioactive phenolics [19]. It suggested the potential of soymilk as a nano-carrier for phenolics.

Increase of H_o suggested that the cavitation effect induced by ultrasound could weaken the hydrogen bonds and intermolecular force, ultimately resulting in the unfolding of protein molecules and exposure of hydrophobic amino acids, which were initially buried within the protein structure [18]. Additionally, protein unfolding might cause by the shear stress induced by ultrasound, thereby increasing the exposure of hydrophobic groups in the proteins [20]. The increased H_o of soymilk suggested that ultrasound treatment could alter their tertiary structure.

3.3. Effect of ultrasound treatment on the secondary structure

As shown in Table 1, ultrasound could affect the secondary structure of soymilk. With ultrasound time increasing, the percentage of β-sheet decreased from 42.41 % to 36.60 %, while the percentage of random coil increased gradually from 28.31 % to 32.83 %, both in a time-dependent manner. Additionally, the percentage of α-helix and β-turn increased

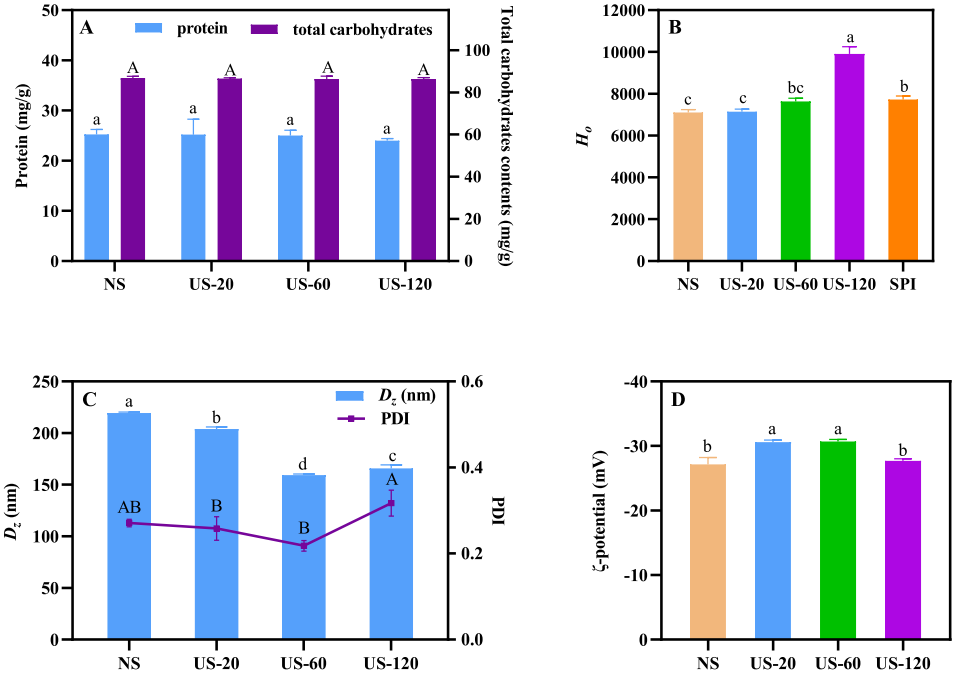

Fig. 1. Effects of ultrasound treatment on the physicochemical properties and structural characteristics of soymilk. (A) Protein and total polysaccharides contents; (B) Surface hydrophobicity (H_o); (C) Z-average diameter (D_z) and PDI; (D) ζ-potential. Values with different letters indicate significantly different at $p < 0.05$.

Table 1
Secondary structural content of soymilk after ultrasound treatment.

	NS	US-20	US-60	US-120
α-Helix (%)	13.36	15.75	15.63	14.78
β-Sheet (%)	42.41	37.72	37.48	36.60
β-Turn (%)	15.92	16.31	16.19	15.79
Random coil (%)	28.31	30.22	30.70	32.83

after treatment for a shorter time (20 min) whereas decreased for a longer treating time (60–120 min). The same trend for the percentages of α-helix and random coil was found in ultrasound-treated soybean proteins [21]. However, previous studies showed an increase in β-sheet and a decrease in random coils, α-helix and β-turn of soymilk after ultrasound treatment (25 kHz, 400 W, 16 min) [9]. These secondary structure changes induced by ultrasound differentiated from our present results. The contradictory results might be due to different treatment conditions, such as ultrasonic power. Previous report revealed that an increase in the β-sheet, but a reduction in the random coils and α-helix was observed when a low power (200–400 W) was used, whereas a reversal result was found when the ultrasonic power increased to 600 W [9,10], which was consistent with present results.

These conformational changes of soymilk may result from the mechanical vibration generated by ultrasound, leading to the collision of protein molecules and the destruction of interactions between molecules [10]. An increase in proportion of α-helix indicated a more compact structure in ultrasound-treated soymilk, as α-helix was regarded as the most tightly integrated structure in proteins [21]. This phenomenon was consistent with the observation of Cryo-SEM. Additionally, hydrophobic interactions of proteins was highly related to the β-sheet proportion. In this way, the decrease in the β-sheet percentage implied that the hydrophobicity was increased due to the exposure of hydrophobic sites inside the molecule [22]. This phenomenon was consistent with the results of H_o. Moreover, the secondary structures of protein is affected by various factors, which included the amino acids sequence, protein property, the interactions between different parts of molecule, aggregation state, degree of denaturation and ultrasound condition. The above results indicated that ultrasound treatment could disrupt some conditions, resulting in secondary structure changes.

3.4. Effects of ultrasound treatment on particle size distribution, ζ-potential and PDI of soymilk

The effects of ultrasound time on the z-average diameter (D_z), PDI and ζ-potential of soymilk was studied. As displayed in Fig. 1C, the D_z of US-20, US-60 and US-120 was 203.83, 159.23 and 165.63 nm, respectively, which were significantly ($p < 0.05$) lower than that of NS (219.47 nm), indicating that ultrasound can significantly reduce the D_z of soymilk. In addition, PDI firstly decreased and then increased as the ultrasound time increased (Fig. 1C). While no significant ($p > 0.05$) differences were observed between NS and US-120. The ζ-potential might act as an indication, which reflected the potential stability of an emulsion system [23]. As shown in Fig. 1D, the ζ-potential (absolute value) of NS was 27.13 mV. This value increased after ultrasound as the repulsion between the particles increased [22]. However, a decrease was observed between the absolute ζ-potential value of US-120 and US-60.

Mu et al. found that ultrasound (20 kHz at 400 W for 9 min) could decrease the particle size and instability index, but increase the absolute value of ζ-potential of soymilk [8]. However, the reduced particle sizes reported by Mu et al. were higher than that of present work. Previous study also found a significant reduction in D_z of soy proteins solution after ultrasound treatment for 15 min [24]. Additionally, the prolonged ultrasound time would cause extended turbulent flow, which could also lead to D_z reduction, and finally resulted in a serious disruption of particles [25]. The reduced particle size induced by ultrasound might be due to the improvement of emulsifying properties resulted from turbulent forces, microstreaming and acoustic cavitation [8]. Similar phenomenon was found for US-20 and US-60. However, significant increases in D_z and PDI were observed in US-120, when compared to US-20 and US-60, implying a possible tendency of reaggregation after longer treatment. Sui et al. [25] pointed out that the increased absolute value of the ζ-potential indicated a high energy barrier between droplets, which could improve the stability of the system as strong electrostatic repulsion occurred. Ultrasound might contribute to the depolymerization of soymilk, leading to the exposure of more negative charges to the surface of particulates. Thereby, a strong repulsion leads to decreased particle size and more stable system [22]. However, a longer time would affect such depolymerization.

3.5. Characterization of the icariin-soymilk nanocomplexes (ISNCs)

3.5.1. EE and LC

Before centrifugation, icariin was quickly precipitated in pure water (WI), while ISNCs showed uniformly dispersed suspension. After centrifugation, the supernatant of WI was transparent and colorless, while all the ISNCs had a homogenous creamy white appearance with a slight yellow tinge, indicating that icariin successfully entered the soymilk and encapsulated (Fig. 2A). As shown in Fig. 2B, the EEs of icariin in ISNCs varied from 85.67 % (USI-120) to 89.67 % (USI-20). Moreover, the LCs of icariin in NSI, USI-20, USI-60 and USI-120 were 28.41, 28.92, 28.22 and 27.64 μg/mg, respectively. These results indicated that ultrasound treatment with an appropriate time could significantly improve EE and LC of icariin ($p < 0.05$). However, such promotion would be reversed when a longer time (60 and 120 min) was applied. Our results indicated that the nanocomplexes could significantly ($p < 0.05$) enhance the solubility of icariin in water (715–749 vs 39.03 μg/mL).

Nano delivery systems have been proven to be effective for the application plant bioactivies [26,27]. Our results indicated that soymilk was a potent nano-carrier for icariin delivery. UHPLC results showed that the LC of ISNCs varied from 2.76 to 2.89 %, higher than that of icariin nanogels (2.03 %) using Span 80 and Tween 80 as nano-carrier [4]. Generally, a higher H_o indicates an improvement of LC in protein, as a higher H_o reflects more hydrophobic binding points at the protein surface available for the binding [19]. However, the increased H_o in US-120 did not improve its LC for icariin. The reduction of EE might result from the folding and aggregation of proteins after excessive ultrasound treatment. Moreover, the opening up protein structures induced by ultrasound might result in more amide bonds to bind to hydrogen bonds, which might affect the encapsulation [28]. However, a higher EE might attribute to the larger size particles, since more volume to surface ratio and less compactness might provide more opportunity for icariin to enter the particle [29].

3.5.2. Particle size distribution and ζ-potential

In general, incorporation of icariin increased the particle size of ISNCs. However, our results revealed that significant ($p < 0.05$) reductions in D_z were observed between USIs (USI-20, USI-60 and USI-120) and corresponding soymilk (Fig. 2C). These results might be due to a tighter structure was formed after encapsulation. The higher D_z of the WI implied the aggregation of icariin in water, which was further confirmed by the PDI value (0.98 ± 0.03) and appearance (Fig. 2A). In addition, the ζ-potentials of the USI-20 and USI-60 were more negative than that of the corresponding soymilk (Fig. 2D). The increase in the negative charges on the surface of nanocomplexes might provide an electrostatic repulsion for the system, which assists to maintain the distance between the particles and leads to a D_z reduction [30].

3.5.3. Morphology

As shown in Fig. 3, the rough surface and multilayer sheet structures were observed on the cross-section of NS. In addition, NS showed a fragmented morphology in different sizes. By comparing with NS, the

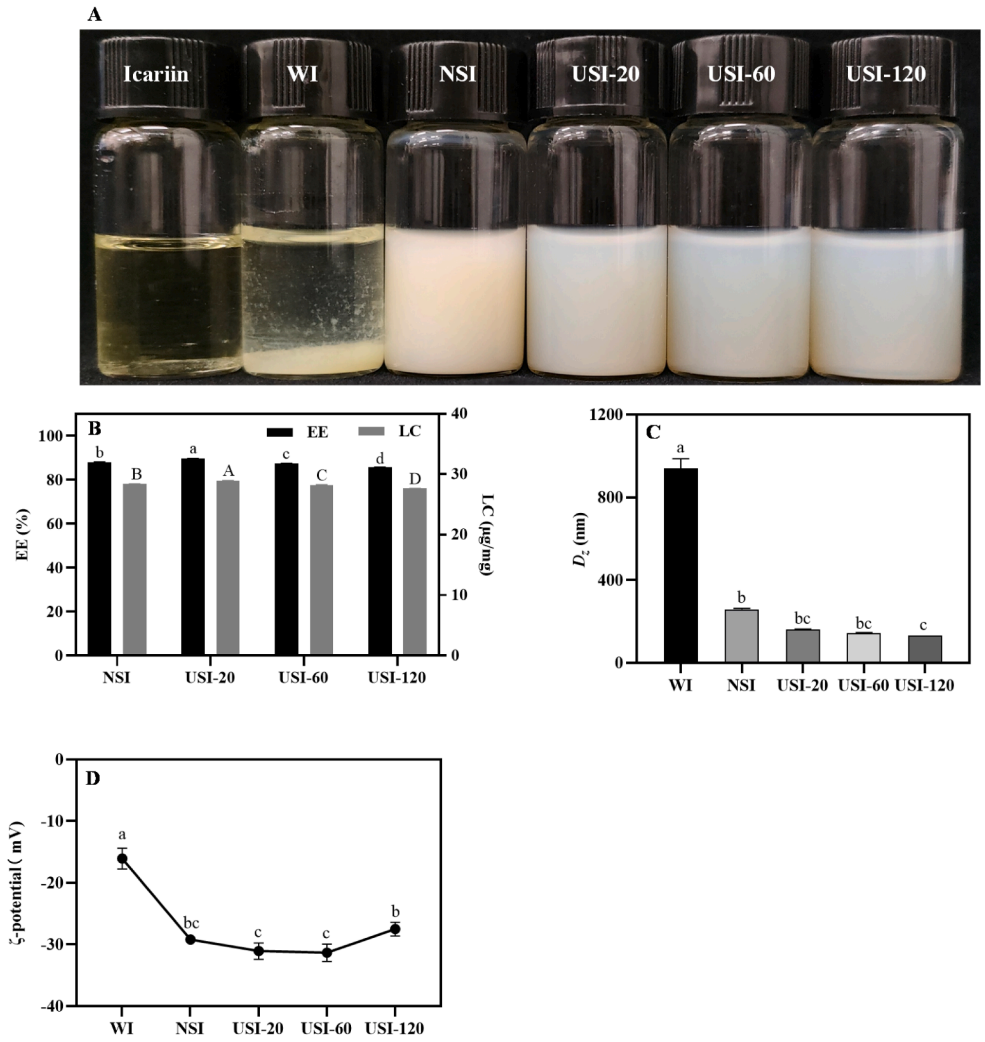

Fig. 2. The characterization of the icariin-soymilk nanocomplexes (ISNCs). (A) The appearances of ISNCs; (B) Encapsulation efficiency (EE) and loading capacity (LC); (C) Z-average diameter (D_z); (D) ζ-potential. Values with no letters in common indicate significant difference at $p < 0.05$.

layered network of ultrasound treated-soymilk seems to be more obvious and thinner. Additionally, the smoother surface of the layered network was visible with ultrasound time increasing. However, tear was observed, especially in US-20. Meanwhile, the structure of US-60 was more compact, which was in agreement with the particle size (Fig. 1C). With increasing ultrasound time, the connection between the micropores of soymilk was destroyed, whereas some short rod-like or point-like structures were visible on the surface, and these structures gradually became more regular. The impact, shear and cavitation effects generated by ultrasound might be due to such phenomenon, as these effects might break down the entanglement between molecules, leading to disruption of the network structure. In addition, previous study showed that significant change in the microstructure of the protein in soy-whey emulsion was induced by ultrasound, thereby assisting to improve the gelation of emulsion [31]. Therefore, the microstructural changes induced by ultrasound might be beneficial for the improvement of functional properties of soymilk.

The icariin exhibited an irregular flocculent structure, connecting by a large number of fine spherical particles. A little amount of icariin was dissolved in water, and little flocculent and loose structure was visible in WI. After binding, the surface of ISNCs became rougher. Moreover, the regular layer and short rod-like or point-like structure in ultrasound-treated soymilk were absent instead of numerous voids and loose structure after encapsulation. The different microstructure of ISNCs and their corresponding soymilk indicated that icariin was well dispersed in soymilk.

3.6. Interaction between soymilk and icariin in ISNCs

3.6.1. NMr

NMR analysis was used to reveal the possible groups of icariin involved in interaction with macromolecules in soymilk. NMR spectra were recorded in both DMSO-d_6 and D_2O solvents. When DMSO-d_6 was used as solvent, both bound icariin in ISNCs and free icariin were visible with obvious signals (Fig. 4). The proton signals of free icariin were 6.64 (6-H), 3.44 (11-H), 3.57 ((11-H), 5.17 (12-H), 1.69 (14-H), 1.60 (15-H), 7.13 (3′-H, 5′-H), 7.90 (2′-H, 6′-H), 3.86 (4′-OCH_3), 0.80 (6′'-H), 3.10 (4′'-H), 3.18 (5′'-H), 5.29 (1′'-H), 4.00 (2′'-H), 3.49 (3′'-H), 5.00 (1′''-H), 3.31 (2′'' and 3′''-H), 3.13 (4′''-H), 3.43 (5′''-H), 3.48 (6′''-H), 3.72 (6′''-H) and 12.56 (5-OH) respectively [32]. Most of proton's signal remained constantly expect for the signals of 5-OH and hydroxyl groups in the sugar moieties of icariin, which were absent in the ^1H spectra of ISNCs, when comparing with the ^1H spectra of free icariin. Additionally, the remained constant signals were also observed when compared the HSQC spectra of bound icariin in ISNCs and free icariin (Fig. 4B). The changed microenvironment of bound icariin in ISNCs might attribute to the vanishing proton signals of these hydroxyl groups as they are active hydrogens. Previous report indicated that a new hydrogen bond was generated in icaritin-loaded pectin nanoparticle, between hydroxyl in pectin and 7-OH of icaritin, suggesting the importance of 7-OH of

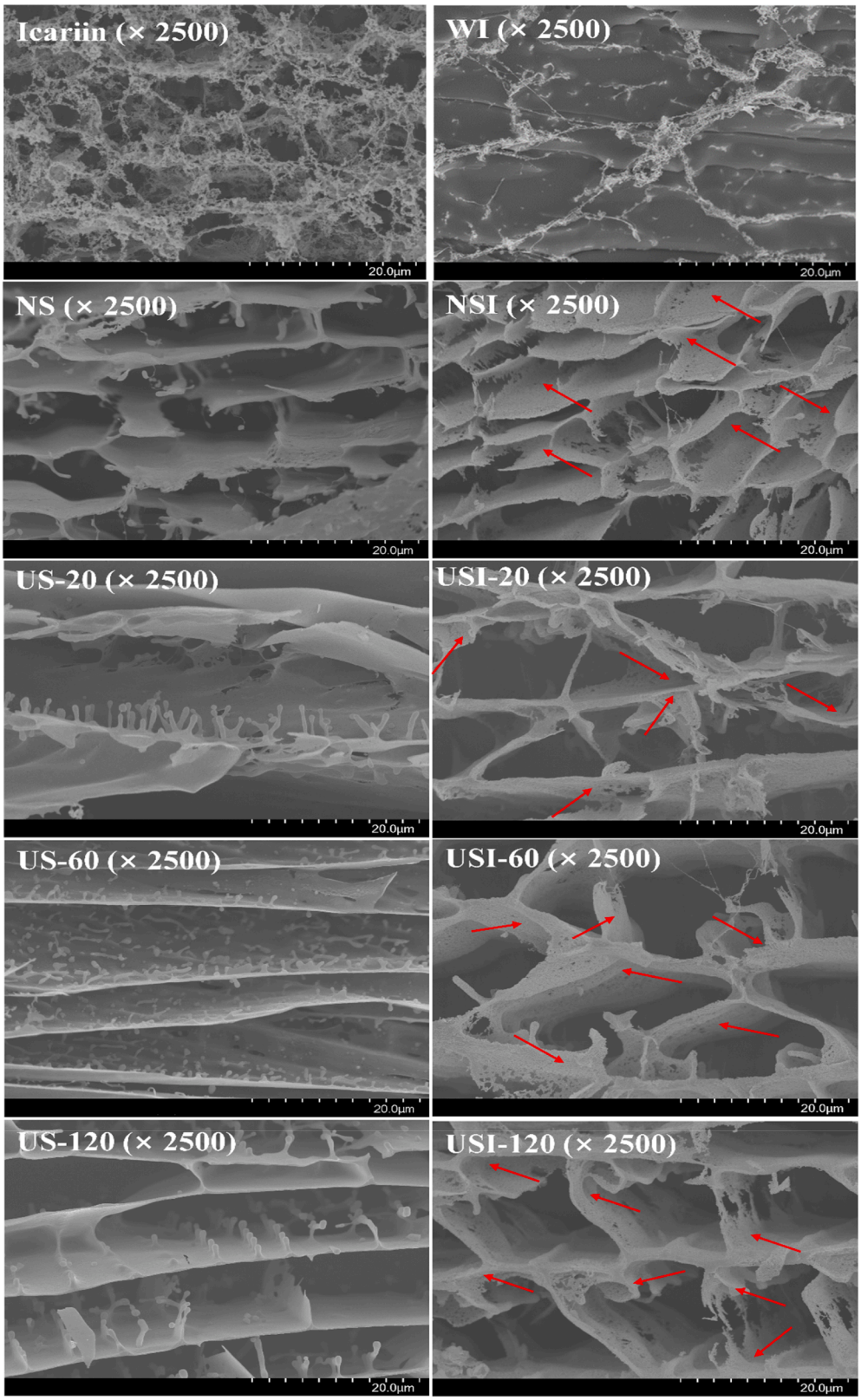

Fig. 3. Cryo-SEM images of icariin, soymilk and ISNCs. Icariin and WI refer to icariin dissolved in 70% ethanol and water, respectively.

icaritin for new hydrogen bond generation [15]. However, as shown in Fig. 4A, the 3-OH and 7-OH in icariin were replaced by rhamnoside and glucoside groups, respectively. Additionally, 5-OH of icariin and hydroxyl in proteins or polysaccharides of soymilk might be hard to form a new hydrogen bond due to the steric hindrance. Previous study indicated that soybean proteins could interact with the hydroxyl groups in starch through hydrogen bonding interaction [33], and higher content of polysaccharides could promote hydrogen bonds generation [34], suggesting the importance of hydroxyl groups in sugar moiety. In the case of other hydroxyl groups in the sugar moieties of icariin, they might

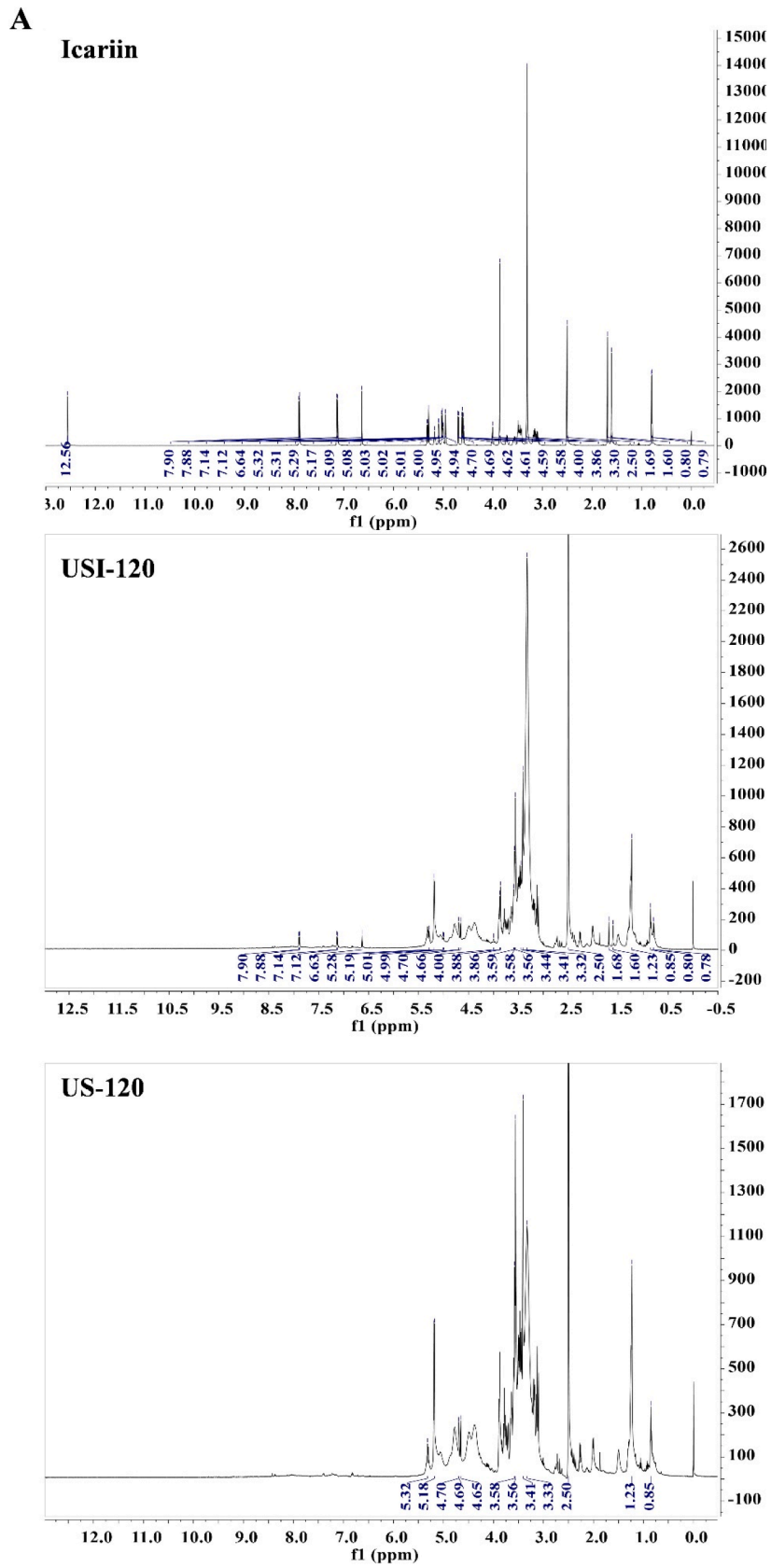

Fig. 4. NMR spectra of icariin, US-120 and USI-120 in DMSO-d_6. (A) ^{1}H spectra; (B) HSQC spectra.

interact with soymilk. However, it is hard to determine whether these hydroxyl groups could interact with soymilk on the basis of vanishing proton signals as the presence of hydrogen exchange. Further study is required to elucidate the generation of new intermolecular bond between hydroxyl groups in the sugar moieties of icariin with soymilk. When D_2O serving as solvent, no signals of icariin could be detected in both ^1H and HSQC spectra (Fig. S1). Only the signals of soymilk were visible and no differences between soymilk in ISNCs and soymilk. These results suggested that icariin might be encapsulated in the hydrophobicity of soymilk.

3.6.2. Fluorescent spectrometry

In Fig. 5A, the fluorescence quenching of soymilk was used to probe the interactions between soymilk and icariin. Without the addition of icariin, soymilk showed the maximum fluorescence intensity at 353 nm. With the increased concentrations of icariin, the maximum fluorescence intensity of the samples gradually weakened. This meant that icariin could interact with soymilk and cause fluorescence quenching. The possible reason was that icariin could bind to hydrophobic patches of soymilk, causing fluorescence burst, and reducing the fluorescence intensity of soymilk [28]. Meanwhile, the obvious blue shift (353–346 nm) suggested that icariin might combine with near the tryptophan residue of soymilk, which could decrease the micro-environmental polarity around tryptophan.

As shown in Table 2, the obtained K_q values were considerably higher than $2 \times 10^{10}\ M^{-1}{\cdot}S^{-1}$ at all the tested temperatures, indicating a static quenching constant was involved. With increasing temperatures, K_{SV} was increased, suggesting that strong hydrophobic interactions were involved in the binding of icariin to soymilk. Similarly, K_A increased with increasing temperatures, suggesting the production of stable ISNCs. In addition, the K_A of soymilk and icariin was between 10^3 and 10^4, belonging to the moderate binding as similar as other ligand–protein interactions [35]. The present results of n values implied that only 1 binding site in the proteins of soymilks working for icariin.

The corresponding thermodynamic parameters might be the main indicators for the main interaction forces involved in the formation of ISNCs. As shown in Table 2, the ΔS and ΔH was above 0, indicating the binding of soymilk and icariin was mainly attributed to hydrophobic interactions. The negative value of ΔG suggested that the binding was a spontaneous process [36]. Generally, once icariin was entered into the hydrophobic interior of soymilk, dehydration of the hydrophobic surfaces might accelerate the complexes formation. This interaction should be accompanied by the release of ordered water molecules, resulting in an unfavorable change in enthalpy ($\Delta H > 0$) and a favorable change in entropy ($\Delta S > 0$), consistent with the classical hydrophobic effect [37]. All these results suggested that ISNCs could be generated through non-covalent interaction forces, and hydrophobic interactions might be mainly involved. In soymilk, proteins mainly present in the form of particles. Icariin might be encapsulated by protein particles through hydrophobic interactions [19]. The pectin-like structure polysaccharides in soymilk might help to improve its encapsulation and stability [38,39].

3.7. Physicochemical stability of nanocomplexes

The stability of nanocomplexes is an important factor affecting its application in food system. In the present work, the ionic strength stability, pH stability, storage stability and thermal stability of nanocomplexes were determined.

3.7.1. Ionic strength stability

The stability of ISNCs among various concentrations of NaCl were determined, using D_z and ζ-potential as indicators. As shown in Fig. 6A, with increasing salt concentration, a significant reduction ($p < 0.01$) in the D_z of NSI was observed. However, significant enhance ($p < 0.01$) in the D_z of USIs was found with increasing salt concentration. Among them, USI-20 and USI-60 were sensitive to the existence of salt ions, even at lower NaCl concentration (200 mM). With more salt addition, the surface charge of all the ISNCs decreased (Fig. 6B). Whereas, no significant ($p > 0.05$) differences were found in the change of the ζ-potential of USI-120 during salt addition, regardless the concentration. These results implied that USI-120 might be relatively resistant to NaCl addition.

The above results indicated that the interactions between ISNCs was influenced by ionic strength, suggesting that electrostatic interactions might be involved in stabilizing ISNCs aggregation. In the absence of salt, the electrostatic repulsion plays a critical role in nanocomplexes against aggregation. In the presence of salt, the interactions such as hydrophobic effects and van der Waals became strong enough to overcome electrostatic interactions [40]. With the increase of salt concentrations, the counter ions, like Cl^- and Na^+ might interfere the surface of ISNCs, leading to partly neutralization of charges, consequently reducing of electrostatic repulsion between ISNCs via electrostatic shielding effect, resulting in the extensive nanocomplexes aggregation [41], which might attribute to D_z increase of USIs. Interestingly, the D_z of USI-120 was consistently lower than that of NSI at all the tested salt concentrations. The dense structure of USI-120 might attribute to this phenomenon, as previous studies revealed that the dense structure of nanoparticles reduced the effects of ionic strength on the interactions between nanoparticles and prohibited their aggregation [42].

3.7.2. pH stability

As shown in Fig. 6C, no obvious changes were observed in the D_z of ISNCs, at pH 6.0–12.0 and 2.0–3.0. However, at pH 4.0–5.0, a large increase in the D_z (>4000 nm) was induced, leading to the formation of sedimentation. The larger D_z could be due to the low electrostatic repulsion between the nanocomplexes [29]. As depicted in Fig. 6D, the changes of ζ-potential were consistent with the results of D_z. The ζ-potential of the ISNCs changed from highly negative at higher pH to highly positive at lower pH, with an isoelectric point around pH 4.5. The soybean protein molecules was mostly responsible for the electrical characteristics of ISNCs [41]. The stability of ISNCs was enhanced attributed to the increase of ζ-potential (absolute value), which contributed to the improvement of electrostatic interaction. In addition, the lower ζ-potential of ISNCs at pH 4.0–5.0 attributed to the weak electrostatic repulsion among ISNCs. Under this condition, ISNCs was unstable and easy to aggregate, which was identical to previous studies, in which curcumin nanoparticles stabilized by proteins aggregated when they lose their charge at a low pH [43]. Overall, our results implied that ISNCs had a smaller size and greater anti-aggregation stability in the pH ranges of 2.0–3.0 and 6.0–12.0, suggesting its promising application in food products.

3.7.3. Storage stability

The long-term stability of ISNCs was investigated by storing at 4 (Fig. 6 E and F) or 25 °C (Fig. 6 G and H) for 28 days. The effects of storage time on the D_z and ζ-potential of the ISNCs were measured. No significant ($p > 0.05$) difference in D_z of USI-60 during 28 days of storage (4 °C), was observed. The D_z of USI-20 and USI-120 decreased within the 14 days and then increased during the last 14 days at 4 °C. On the contrary, the D_z of USIs increased since day 14 when kept at 25 °C. In addition, during the whole storage period, the D_z of NSI was larger than that of USIs. The results indicated that the ISNCs were more stable on storage at 4 °C than at 25 °C, suggesting that lower temperature may be beneficial for extending the storage time of ISNCs.

The ζ-potential of ISNCs slightly changed both at 4 and 25 °C for 28-day storage, with a range of 28–32 mV (absolute values). In addition, no aggregation and flocculation were found during the storage time at both temperatures in all the USIs. However, a small amount of light-yellow sediment formed at the bottom of the tube of NSI since 21st day, especially those at 25 °C (data not shown), indicating that a small amount of icariin in NSI was precipitated during long term storage. Therefore, the

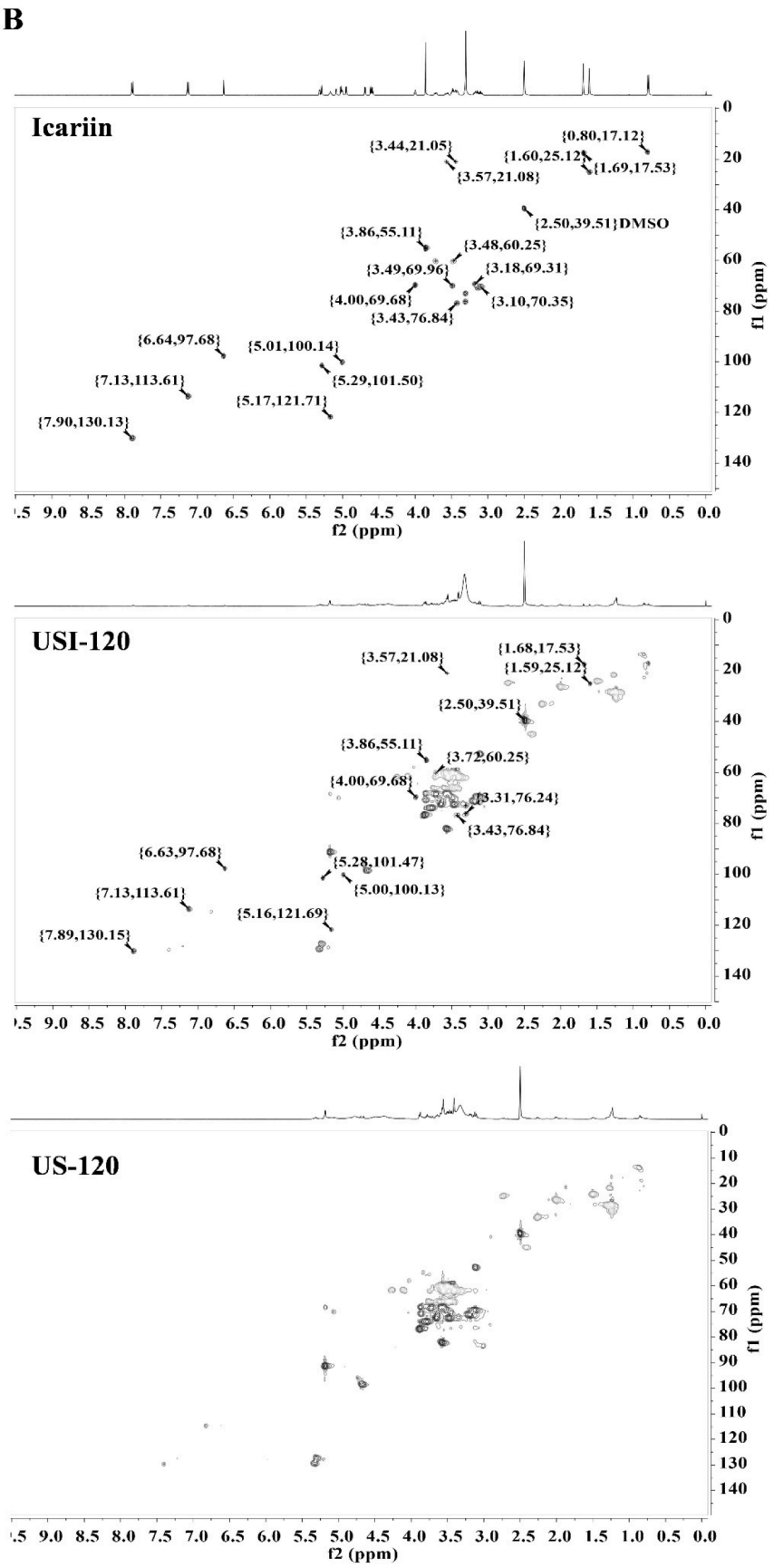

Fig. 5. Interaction between soymilk and icariin in the ISNCs. (A) Fluorescence spectra of ISNCs at 298 K; (B) Stern-Volmer curve and (C) double logarithmic graph derived from fluorescence spectra at different temperatures (298, 303 and 308 K).

Table 2
Binding parameters and thermodynamic parameters for soymilk and icariin at different temperatures.

Temperature (K)	Binding parameters				Thermodynamic parameters		
	K_{SV} ($\times 10^4$ M^{-1})	K_q ($\times 10^{12}$ $M^{-1}S^{-1}$)	K_A ($\times 10^3$ M^{-1})	n	ΔH (KJ·mol^{-1})	ΔS (J·mol^{-1}·k^{-1})	ΔG (KJ·mol^{-1})
298 K	6.85	6.85	2.18	0.64	8.9	37.54	−2.29
303 K	6.87	6.87	3.78	0.69			−2.48
308 K	7.22	7.22	5.30	0.71			−2.67

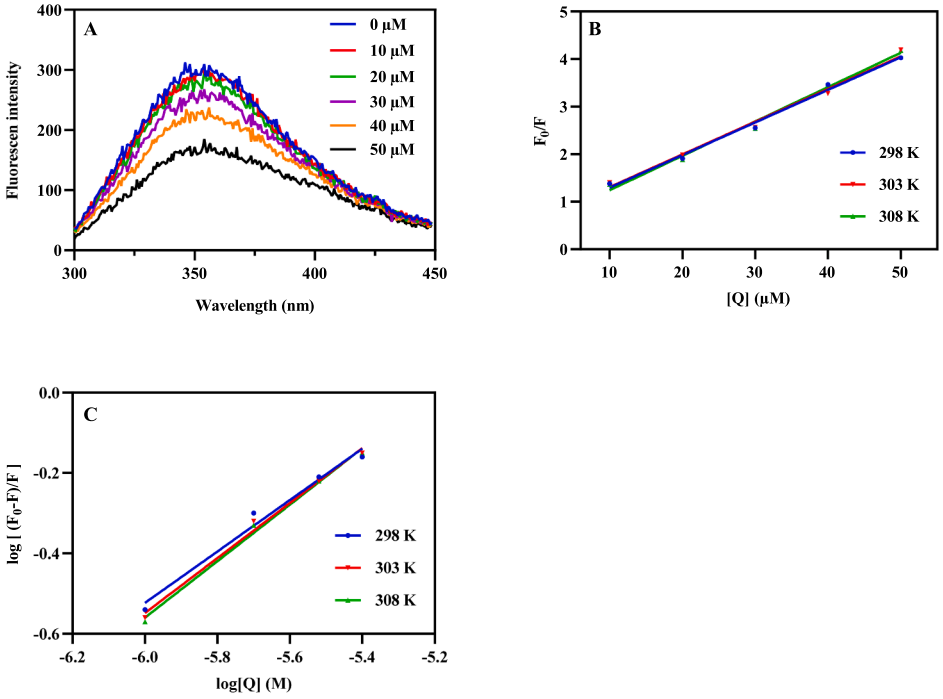

Fig. 6. Physicochemical stability of ISNCs. (A) Effects of pH on the z-average diameter (D_z) and (B) ζ-potential of ISNCs; (C) Effects of NaCl addition on the z-average diameter (D_z) and (D) ζ-potential of ISNCs; (E) Changes in z-average diameter (D_z) and (F) ζ-potential of ISNCs during storage at 4 °C for 28 days; (G) Changes in z-average diameter (D_z) and (H) ζ-potential of ISNCs during storage at 25 °C for 28 days; (I) Retention rate of icariin in NSI, USI-20, USI-60 and USI-120 complex after incubation under different temperature. The significant differences from the corresponding initiate ISNCs are indicated by asterisks, where "*" and "**" refer to significant differences *at* $p < 0.05$ and $p < 0.01$, respectively.

present results implied that USIs exhibited a good storage stability, especially USI-60.

In general, the total number of microorganisms during storage increased rapidly, which might lead to acid-production and an increase in H^+ to neutralize the negative charge of soymilk, resulting in a decrease in the absolute value of ζ-potential and increase of D_z. Previous study showed that acoustic cavitation induced by ultrasound could inhibit microorganisms growth, accelerate oil droplet rupture, and decrease protein aggregation, thus improving the stability of soymilk [8]. Peng et al. [43] also pointed out that curcumin nanoparticles stabilized by proteins exhibited better storage stability, especially those at 4 °C, and the higher affinity of whey protein to curcumin nanoparticles was the main contributor. The present results implied that soymilk-base nanocomplexes was positive in the long term-storage protection for icariin in water matrix.

3.7.4. *Thermal stability*

The stability of icariin in ISNCs under different temperature was investigated using retention rate as an indicator (Fig. 6I). After incubation for 2 h at 25 °C, the retention rate of icariin in the nanocomplexes was 100 %. After heating at 60 °C for 2 h, the retention rate of icariin in NSI, USI-20, USI-60 and USI-120 were 97.74, 97.72, 96.88 and 97.74 %, respectively. While these values slightly decreased to 95.85, 97.31, 95.34 and 97.47 % after incubated at 90 °C for 2 h, respectively. These results indicated that the ISNCs can provide a better protection of icariin during thermal treatment, regardless of temperature.

Similarly, zein-caseinate nanoparticles showed better protection effect for encapsulated curcumin against thermal treatment, where incubating at 180 °C for 40 min resulting in 73.69 % of curcumin remained in the nanoparticles [17]. A possible explanation for this phenomenon was that both steric and electrostatic repulsion between the nanocomplexes were beneficial to enhance the protection of flavonoids against thermal treatment through inhibiting the disintegration or aggregation of nanoparticles [17]. The previous study showed that ultrasonic treatment could improve the thermal stability of soymilk as the smaller particle size and higher ζ-potential (absolute value) could reduce the aggregation of soymilk droplets [8]. Such improvement of thermal stability might contribute to the enhancement for the protective effect of icariin during heat treatment. In addition, previous reports revealed that the interactions between protein-polysaccharide complex could improve the stability of protein-based nanocomplexes under different environmental stress [38]. Therefore, the polysaccharides in soymilk might help to improve the stability of ISNCs. Numerous reports have documented that encapsulation is a promising way to protect bioactive substances from thermal degradation through building physical barrier [43,44].

3.8. *In vitro gastrointestinal digestion*

After simulation in gastric fluids (SGF), the D_z of ISNCs increased, and then decreased after simulated intestinal fluids (SIF) digestion (Fig. 7A). The present results were in agreement with the study of Wang et al. [23]. No significant ($p > 0.05$) change in D_z among NSI, USI-20 and USI-60 in SGF, were observed. Similarly, no significant ($p > 0.05$)

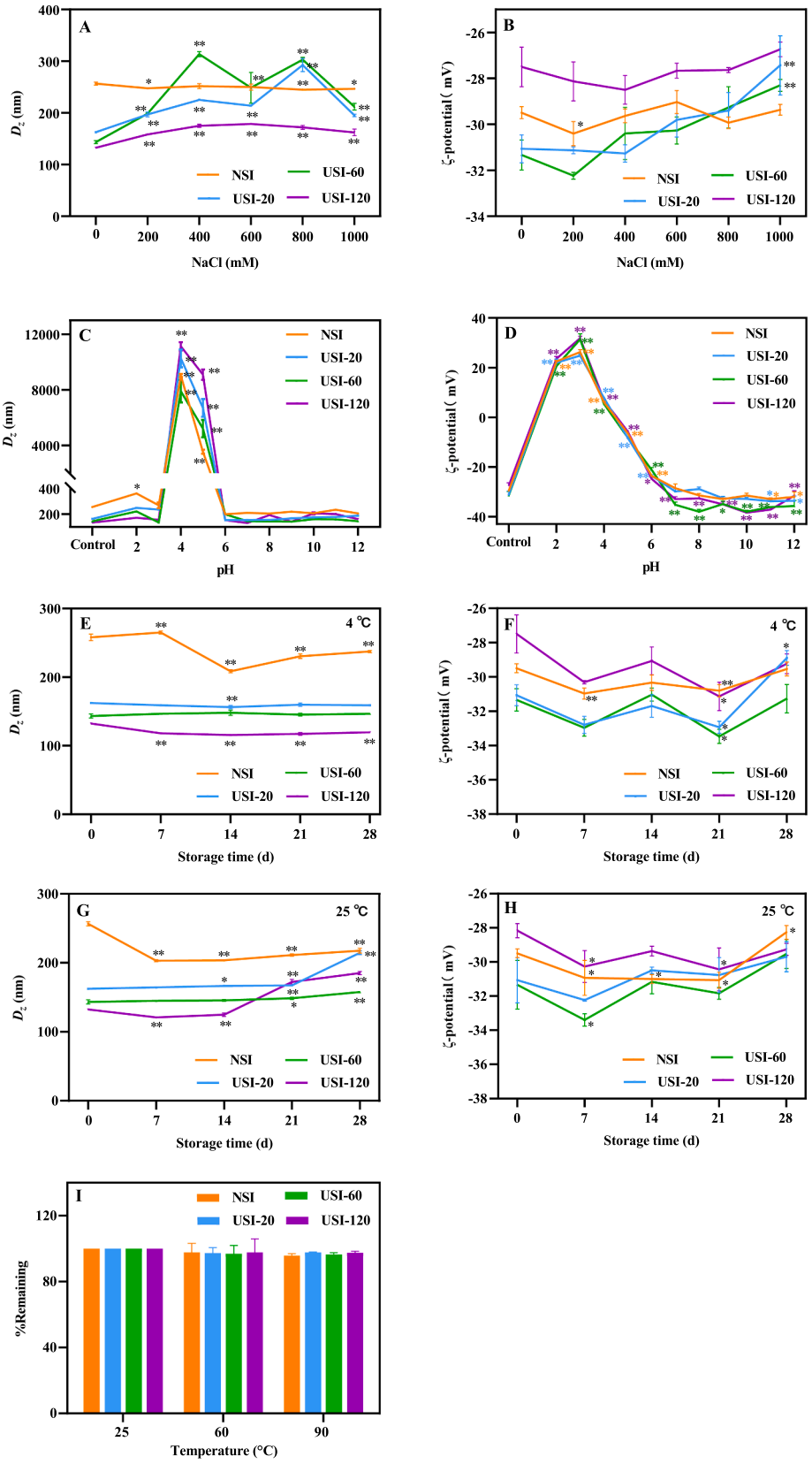

Fig. 7. The stability and bioaccessibilities during *in vitro* gastrointestinal digestion. (A) Z-average diameter (D_z) of WI, NSI, USI-20, USI-60 and USI-120 during *in vitro* digestion; (B) The bioaccessibilities of icariin after simulated gastric-intestinal digestion. Columns with different letters indicate significant difference at $p < 0.05$.

change in D_z in SIF among all the tested samples were found.

The increase in D_z might be due to the electrostatic shielding effect during SGF, which is influenced by pepsin, pH and high ionic strength in SGF [16]. In addition, digestive hydrolysis could reduce the thickness of the protein layer, affect the action of electrostatic repulsion, which might lead to the nanocomplexes binding with pepsin molecules and bridge with adjacent nanocomplexes to form aggregation that increased the D_z [45]. The aggregation formed in SGF has been disaggregated in SIF, resulting from the variation in digestive environment affected the structural properties of pepsin. Reducing the concentration of pepsin will weaken the bridging flocculation effect. Meanwhile, the decrease in D_z during SIF may also be due to the changes in pH and ionic strength, which may alter the electrostatic interactions between ISNCs, collectively exacerbating the disaggregation of nanocomplexes [46].

As displayed in Fig. 7B, free icariin exhibited the lowest bioaccessibility (11.20 % of 39 μg/mL) after SIF. However, the bioaccessibility of icariin in the ISNCs was higher than 58 %. Especially for USI-60, its bioaccessibility reached 76.08 % (of 730 μg/mL), followed by USI-20 (67.44 %). The lower ζ-potentials of USI-60 and USI-20 generally reflects them with relatively higher colloidal stability. The ISNCs might be rapidly hydrolyzed by trypsin during the SIF digestion, and the hydrolysates might be converted into micelles under the cross-linking of bile salts [47]. The micelles formed by USI-60 and USI-120 still have high colloidal stability, which may facilitate absorption in the intestinal tract. The results indicated that the utilization of soymilk to encapsulate icariin was an effective strategy for delivering icariin to the intestine.

The improved bioaccessibility might be due to proteins promoting the transfer of icariin to the mixed micelle phase in the digests [44]. The ISNCs contained some proteins, which could be digested by proteases in SGF to form peptides, which formed micelles or complexes with bile salts in SIF that dissolved icariin [47]. The release of icariin in ISNCs might also be related to the strong ionic strength, enzymes and pH during gastrointestinal digestion, which promoted the dissociation of nanocomplexes [45]. The result was consistent with previous study, in which nanoparticles could significant improve the bioaccessibility of soy isoflavone [44]. These results indicated that ISNCs could be used as an effective technique to deliver icariin.

4. Conclusions

The above results indicated that ultrasound treatment was advantageous to the chemical composition, physical properties and structural characteristics of soymilk. Meanwhile, ISNCs were successfully fabricated and characterized. ISNCs remarkably improved the water solubility (about 20 folds) and storage stability of icariin (>28 days). Ultrasound treatment with a shorter time (20 min) could significantly increase the EE and LC of NSI, leading to the highest EE of 89.67 % and highest LC of 28.92 μg/mg. In addition, ISNCs exhibited better pH stability (ranging from 6.0 to12.0 and from 2.0 to 3.0), ionic strength stability, thermal stability and storage stability. Among them, USI-120 had the smallest particle size (132.47 nm), whereas USI-60 had the lowest ζ-potential (-31.33 mV) and the highest bioaccessibility (76.08 %). Therefore, ultrasound treated-soymilk have a great potential to be utilized as a delivery system for icariin.

CRediT authorship contribution statement

Jinping Wang: Formal analysis, Investigation, Writing – original draft. **Hong Zhu:** Formal analysis. **Yueming Jiang:** Formal analysis, Writing – review & editing. **Jianbo Xiao:** Writing – review & editing. **Bao Yang:** Conceptualization, Supervision, Writing – review & editing. **Lingrong Wen:** Conceptualization, Supervision, Writing – review & editing.

Declaration of Competing Interest

The authors declare that they have no known competing financial interests or personal relationships that could have appeared to influence the work reported in this paper.

Acknowledgements

The authors are grateful to the financial support from Youth Innovation Promotion Association, Chinese Academy of Sciences (No. 2022353) and Science and Technology Planning Project of Guangdong Province (No. 2022A0505050055).

Appendix A. Supplementary data

Supplementary data to this article can be found online at https://doi.org/10.1016/j.ultsonch.2022.106230.

References

[1] C. Li, Q. Li, Q. Mei, T. Lu, Pharmacological effects and pharmacokinetic properties of icariin, the major bioactive component in Herba Epimedii, Life Sci. 126 (2015) 57–68, https://doi.org/10.1016/j.lfs.2015.01.006.
[2] Z. Luo, J. Dong, J. Wu, Impact of Icariin and its derivatives on inflammatory diseases and relevant signaling pathways, Int. Immunopharmacol. 108 (2022), 108861, https://doi.org/10.1016/j.intimp.2022.108861.
[3] R. Szabó, C.P. Rácz, F.V. Dulf, Bioavailability improvement strategies for icariin and its derivates: A review, Int. J. Mol. Sci. 23 (14) (2022) 7519.
[4] D. Xu, Y.R. Lu, N. Kou, M.J. Hu, Q.S. Wang, Y.L. Cui, Intranasal delivery of icariin via a nanogel-thermoresponsive hydrogel compound system to improve its antidepressant-like activity, Int. J. Pharm. 586 (2020), 119550, https://doi.org/10.1016/j.ijpharm.2020.119550.
[5] K. Rahmati, M. Mazaheri Tehrani, K. Daneshvar, Soy milk as an emulsifier in mayonnaise: physico-chemical, stability and sensory evaluation, J. Food Sci. Technol. 51 (11) (2014) 3341–3347, https://doi.org/10.1007/s13197-012-0806-9.
[6] B. Zheng, H. Lin, X. Zhang, D.J. McClements, Fabrication of curcumin-loaded dairy milks using the pH-shift method: Formation, stability, and bioaccessibility, J. Agric. Food Chem. 67 (44) (2019) 12245–12254, https://doi.org/10.1021/acs.jafc.9b04904.
[7] C. Zhao, Z. Chu, Z. Miao, J. Liu, J. Liu, X. Xu, Y. Wu, B. Qi, J. Yan, Ultrasound heat treatment effects on structure and acid-induced cold set gel properties of soybean protein isolate, Food Biosci. 39 (2021), 100827, https://doi.org/10.1016/j.fbio.2020.100827.
[8] Q. Mu, H. Su, Q. Zhou, S. Xiao, L. Zhu, X. Xu, S. Pan, H. Hu, Effect of ultrasound on functional properties, flavor characteristics, and storage stability of soybean milk, Food Chem. 381 (2022), 132158, https://doi.org/10.1016/j.foodchem.2022.132158.
[9] S.K. Vanga, J. Wang, V. Raghavan, Effect of ultrasound and microwave processing on the structure, in-vitro digestibility and trypsin inhibitor activity of soymilk proteins, LWT-Food Sci. Technol. 131 (2020), 109708, https://doi.org/10.1016/j.lwt.2020.109708.
[10] L. Zhang, X. Wang, Y. Hu, O. Abiola Fakayode, H. Ma, C. Zhou, Z. Hu, A. Xia, Q. Li, Dual-frequency multi-angle ultrasonic processing technology and its real-time monitoring on physicochemical properties of raw soymilk and soybean protein, Ultrason. Sonochem. 80 (2021), 105803, https://doi.org/10.1016/j.ultsonch.2021.105803.
[11] H. Hu, X. Zhu, T. Hu, I.W.Y. Cheung, S. Pan, E.C.Y. Li-Chan, Effect of ultrasound pre-treatment on formation of transglutaminase-catalysed soy protein hydrogel as a riboflavin vehicle for functional foods, J. Funct. Foods 19 (2015) 182–193, https://doi.org/10.1016/j.jff.2015.09.023.
[12] I.D. Nwachukwu, R.E. Aluko, A systematic evaluation of various methods for quantifying food protein hydrolysate peptides, Food Chem. 270 (2019) 25–31, https://doi.org/10.1016/j.foodchem.2018.07.054.
[13] L. Wen, L. Lin, L. You, B. Yang, G. Jiang, M. Zhao, Ultrasound-assited extraction and structural identification of polysaccharides from *Isodon lophanthoides* var. gerardianus (Bentham) H. Hara, Carbohydr. Polym. 85 (3) (2011) 541–547, https://doi.org/10.1016/j.carbpol.2011.03.003.
[14] J. Wang, J. Liu, A. John, Y. Jiang, H. Zhu, B. Yang, L. Wen, Structure identification of walnut peptides and evaluation of cellular antioxidant activity, Food Chem. 388 (2022), 132943, https://doi.org/10.1016/j.foodchem.2022.132943.
[15] Y. Chen, Y. Jiang, L. Wen, B. Yang, Structure, stability and bioaccessibility of icaritin-loaded pectin nanoparticle, Food Hydrocoll. 129 (2022), 107663, https://doi.org/10.1016/j.foodhyd.2022.107663.
[16] L. Dai, Y. Wei, C. Sun, L. Mao, D.J. McClements, Y. Gao, Development of protein-polysaccharide-surfactant ternary complex particles as delivery vehicles for curcumin, Food Hydrocoll. 85 (2018) 75–85, https://doi.org/10.1016/j.foodhyd.2018.06.052.
[17] J. Xue, Y. Zhang, G. Huang, J. Liu, M. Slavin, L. Yu, Zein-caseinate composite nanoparticles for bioactive delivery using curcumin as a probe compound, Food Hydrocoll. 83 (2018) 25–35, https://doi.org/10.1016/j.foodhyd.2018.04.037.

[18] R. Liu, Q. Liu, S.B. Xiong, Y.C. Fu, L. Chen, Effects of high intensity unltrasound on structural and physicochemical properties of myosin from silver carp, Ultrason. Sonochem. 37 (2017) 150–157, https://doi.org/10.1016/j.ultsonch.2016.12.039.
[19] F.P. Chen, B.S. Li, C.H. Tang, Nanocomplexation between curcumin and soy protein isolate: Influence on curcumin stability/bioaccessibility and *in vitro* protein digestibility, J. Agric. Food Chem. 63 (13) (2015) 3559–3569, https://doi.org/10.1021/acs.jafc.5b00448.
[20] A. Miklavzin, M. Cegnar, J. Kerc, J. Kristl, Effect of surface hydrophobicity of therapeutic protein loaded in polyelectrolyte nanoparticles on transepithelial permeability, Acta Pharm. 68 (3) (2018) 275–293, https://doi.org/10.2478/acph-2018-0032.
[21] H. Hu, J. Wu, E.C.Y. Li-Chan, L. Zhu, F. Zhang, X. Xu, G. Fan, L. Wang, X. Huang, S. Pan, Effects of ultrasound on structural and physical properties of soy protein isolate (SPI) dispersions, Food Hydrocoll. 30 (2) (2013) 647–655, https://doi.org/10.1016/j.foodhyd.2012.08.001.
[22] Q. Cui, L. Wang, G. Wang, A. Zhang, X. Wang, L. Jiang, Ultrasonication effects on physicochemical and emulsifying properties of *Cyperus esculentus* seed (tiger nut) proteins, LWT-Food Sci. Technol. 142 (2021), 110979, https://doi.org/10.1016/j.lwt.2021.110979.
[23] Y. Wang, W. Jiang, Y. Jiang, D. Julian McClements, F. Liu, X. Liu, Self-assembled nano-micelles of lactoferrin peptides: Structure, physicochemical properties, and application for encapsulating and delivering curcumin, Food Chem. (2022), 132790, https://doi.org/10.1016/j.foodchem.2022.132790.
[24] A.R. Jambrak, V. Lelas, T.J. Mason, G. Krešić, M. Badanjak, Physical properties of ultrasound treated soy proteins, J. Food Eng. 93 (4) (2009) 386–393, https://doi.org/10.1016/j.jfoodeng.2009.02.001.
[25] X. Sui, S. Bi, B. Qi, Z. Wang, M. Zhang, Y. Li, L. Jiang, Impact of ultrasonic treatment on an emulsion system stabilized with soybean protein isolate and lecithin: Its emulsifying property and emulsion stability, Food Hydrocoll. 63 (2017) 727–734, https://doi.org/10.1016/j.foodhyd.2016.10.024.
[26] E. Jagtiani, Advancements in nanotechnology for food science and industry, Food Frontiers 3 (1) (2022) 56–82, https://doi.org/10.1002/fft2.104.
[27] S. Caballero, Y.O. Li, D.J. McClements, G. Davidov-Pardo, Encapsulation and delivery of bioactive citrus pomace polyphenols: a review, Crit. Rev. Food Sci. Nutr. 62 (29) (2022) 8028–8044.
[28] X. Luo, F. Fan, X. Sun, P. Li, T. Xu, J. Ding, Y. Fang, Effect of ultrasonic treatment on the stability and release of selenium-containing peptide TSeMMM-encapsulated nanoparticles *in vitro* and *in vivo*, Ultrason. Sonochem. 83 (2022), 105923, https://doi.org/10.1016/j.ultsonch.2022.105923.
[29] Z. Li, Q. Lin, D.J. McClements, Y. Fu, H. Xie, T. Li, G. Chen, Curcumin-loaded core-shell biopolymer nanoparticles produced by the pH-driven method: Physicochemical and release properties, Food Chem. 355 (2021), 129686, https://doi.org/10.1016/j.foodchem.2021.129686.
[30] S. Zhou, L. Han, K. Lu, B. Qi, X. Du, G. Liu, Y. Tang, S. Zhang, Y. Li, Whey protein isolate-phytosterols nanoparticles: Preparation, characterization, and stabilized food-grade pickering emulsions, Food Chem. 384 (2022), 132486, https://doi.org/10.1016/j.foodchem.2022.132486.
[31] Q. Cui, X. Wang, G. Wang, R. Li, X. Wang, S. Chen, J. Liu, L. Jiang, Effects of ultrasonic treatment on the gel properties of microbial transglutaminase crosslinked soy, whey and soy–whey proteins, Food Sci. Biotechnol. 28 (5) (2019) 1455–1464, https://doi.org/10.1007/s10068-019-00583-y.
[32] Q. Xia, D. Xu, Z. Huang, J. Liu, X. Wang, X. Wang, S. Liu, Preparation of icariside II from icariin by enzymatic hydrolysis method, Fitoterapia 81 (5) (2010) 437–442, https://doi.org/10.1016/j.fitote.2009.12.006.
[33] Z. Lu, Y. Liu, Y.E.J. Lee, A. Chan, P.-R. Lee, H. Yang, Effect of starch addition on the physicochemical properties, molecular interactions, structures, and in vitro digestibility of the plant-based egg analogues, Food Chem. 403 (2023), 134390, https://doi.org/10.1016/j.foodchem.2022.134390.
[34] X. Ran, X. Lou, H. Zheng, Q. Gu, H. Yang, Improving the texture and rheological qualities of a plant-based fishball analogue by using konjac glucomannan to enhance crosslinks with soy protein, Innov. Food Sci. Emerg. Technol. 75 (2022), 102910, https://doi.org/10.1016/j.ifset.2021.102910.
[35] H. Li, Y. Yuan, J. Zhu, T. Wang, D. Wang, Y. Xu, Zein/soluble soybean polysaccharide composite nanoparticles for encapsulation and oral delivery of lutein, Food Hydrocoll. 103 (2020), 105715, https://doi.org/10.1016/j.foodhyd.2020.105715.
[36] C. Fan, J.-L. Yuan, J. Guo, X. Kang, Soy protein isolate (SPI)-hemin complex nanoparticles as a novel water-soluble iron-fortifier: Fabrication, formation mechanism and *in vitro* bioavailability, Food Biosci. 49 (2022), 101889, https://doi.org/10.1016/j.fbio.2022.101889.
[37] B.K. Paul, Classical vs. nonclassical hydrophobic interactions underlying various interaction processes: Application of isothermal titration calorimetry, Chem. Phys. Impact 5 (2022) pp, https://doi.org/10.1016/j.chphi.2022.100104.
[38] C. Shen, W. Chen, C. Li, X. Chen, H. Cui, L. Lin, Pickering emulsion stabilized by gliadin/soybean polysaccharide composite colloidal nanoparticle: Physicochemical properties and its application on washing of fresh-cut cabbage, Food Res. Int. 161 (2022), 111886, https://doi.org/10.1016/j.foodres.2022.111886.
[39] Z. Lu, P.-R. Lee, H. Yang, Chickpea flour and soy protein isolate interacted with κ-carrageenan via electrostatic interactions to form egg omelets analogue, Food Hydrocoll. 130 (2022), 107691, https://doi.org/10.1016/j.foodhyd.2022.107691.
[40] L. Dai, C. Sun, R. Li, L. Mao, F. Liu, Y. Gao, Structural characterization, formation mechanism and stability of curcumin in zein-lecithin composite nanoparticles fabricated by antisolvent co-precipitation, Food Chem. 237 (2017) 1163–1171, https://doi.org/10.1016/j.foodchem.2017.05.134.
[41] K. Hu, D.J. McClements, Fabrication of surfactant-stabilized zein nanoparticles: A pH modulated antisolvent precipitation method, Food Res. Int. 64 (2014) 329–335, https://doi.org/10.1016/j.foodres.2014.07.004.
[42] X. Wang, M. Li, F. Liu, F. Peng, F. Li, X. Lou, Y. Jin, J. Wang, H. Xu, Fabrication and characterization of zein-tea polyphenols-pectin ternary complex nanoparticles as an effective hyperoside delivery system: Formation mechanism, physicochemical stability, and *in vitro* release property, Food Chem. 364 (2021), 130335, https://doi.org/10.1016/j.foodchem.2021.130335.
[43] S. Peng, L. Zhou, Q. Cai, L. Zou, C. Liu, W. Liu, D.J. McClements, Utilization of biopolymers to stabilize curcumin nanoparticles prepared by the pH-shift method: Caseinate, whey protein, soy protein and gum arabic, Food Hydrocoll. 107 (2020), 105963, https://doi.org/10.1016/j.foodhyd.2020.105963.
[44] Q. Liu, Y. Sun, J. Cheng, M. Guo, Development of whey protein nanoparticles as carriers to deliver soy isoflavones, LWT-Food Sci. Technol. 155 (2022), 112953, https://doi.org/10.1016/j.lwt.2021.112953.
[45] X. Li, P. Zhou, Z. Luo, R. Feng, L. Wang, Hohenbuehelia serotina polysaccharides self-assembled nanoparticles for delivery of quercetin and their anti-proliferative activities during gastrointestinal digestion *in vitro*, Int. J. Biol. Macromol. 203 (2022) 244–255, https://doi.org/10.1016/j.ijbiomac.2022.01.143.
[46] Y. Yuan, M. Ma, S. Zhang, D. Wang, Y. Xu, pH-driven self-assembly of alcohol-free curcumin-loaded propylene glycol alginate nanoparticles, Int. J. Biol. Macromol. 195 (2022) 302–308, https://doi.org/10.1016/j.ijbiomac.2021.12.025.
[47] Q. Liu, Y. Sun, Q. Cui, J. Cheng, A. Killpartrik, A.H. Kemp, M. Guo, Characterization, antioxidant capacity, and bioaccessibility of Coenzyme Q10 loaded whey protein nanoparticles, LWT-Food Sci. Technol. 160 (2022), 113258, https://doi.org/10.1016/j.lwt.2022.113258.